Scanning tunneling microscopy identification of van Hove singularities and negative thermal expansion in highly oriented pyrolytic graphite with hexagonal moiré superlattices

Filippo S.Boi , Ayoub Taallah , Shuai Gao , Jian Guo , Shanling Wang , Anna Corrias

PII: S2667-0569(21)00011-0
DOI: https://doi.org/10.1016/j.cartre.2021.100034
Reference: CARTRE 100034

To appear in: *Carbon Trends*

Received date: 23 December 2020
Revised date: 28 January 2021
Accepted date: 29 January 2021

Please cite this article as: Filippo S.Boi , Ayoub Taallah , Shuai Gao , Jian Guo , Shanling Wang , Anna Corrias , Scanning tunneling microscopy identification of van Hove singularities and negative thermal expansion in highly oriented pyrolytic graphite with hexagonal moiré superlattices, *Carbon Trends* (2021), doi: https://doi.org/10.1016/j.cartre.2021.100034

Scanning tunneling microscopy identification of van Hove singularities and negative thermal expansion in highly oriented pyrolytic graphite with hexagonal moiré superlattices

Filippo S. Boi [a*], Ayoub Taallah[a], Shuai Gao[a], Jian Guo[a], Shanling Wang[b*] and Anna Corrias[*c].

a. College of Physics, Sichuan University, Chengdu, China

b. Analytical and Testing Center, Sichuan University, Chengdu, China

c. School of Physical Sciences, University of Kent, Canterbury, UK CT2 7NZ.

Corresponding authors: f.boi@scu.edu.cn, wangshanling@scu.edu.cn, a.corrias@kent.ac.uk

Abstract

We report a novel investigation on the structural, electronic and magnetic properties of highly-oriented-pyrolytic-graphite (HOPG) by employing STM/S, TEM and SQUID. Van Hove singularities (vHs) were identified by STS-acquisition of local-density-of-states spectra (LDOS) acquired from moiré-superlattice-periodicities D ~0.5 nm (θ_{rot} ~28.6º), ~2 nm (θ_{rot} of ~7.08º) and ~ 4 nm (θ_{rot} ~3.6º). A possible interlayer-coupling- or moiré-thickness-induced variation of the vHs-separation-parameter was identified. Investigation of the spatial-distribution of the moiré-superlattices by exfoliation revealed also D ~13.87 nm (θ_{rot} ~1.02º), ~13.0 nm (θ_{rot} ~1.09º), ~12.65 nm (θ_{rot} ~1.12º) and ~2.03 nm (θ_{rot} ~7.0º). These observations were further supported by additional LDOS spectra acquired on HOPG from moiré-superlattice-periodicities D ~8 nm (θ_{rot} ~1.8º). In the latter, the unusual presence of four vHs peaks evidenced the existence of multiple rotational effects between internal sublattices. Extended analyses were further performed by T-XRD from 12K to 298K. Unknown peak-features exhibiting unusual T-dependent shifts were analysed at $2\theta \sim 21^{\circ}$ (Fig.6A-C) and ~ 43° (Fig.6D). ZFC and FC-signals from the exfoliated lamellae further evidenced an anisotropic ferromagnetic behaviour, possibly involving the coexistence of 1) disorder induced percolative ferromagnetism and 2) additional magnetic components arising from the locally twisted sublattices, which were found to exhibit the moiré superlattices.

1 Introduction

The recent observations of superconductive and ferromagnetic phenomena in twisted bilayer graphene have attracted significant attention in the areas of condensed matter physics and materials science [1-6]. Presence of rotational misorientation ($1° \leq \theta_{twist} \leq 10°$) between graphene layers gives rise to moiré superlattices with consequent appearance of van Hove singularities (vHs) in the local density of states (LDOS) spectra acquired with scanning tunnelling spectroscopy (STS). [1-10]. Interestingly, vHs peaks were successfully identified already in 2010 by Li et al. in LDOS spectra acquired from hexagonal moiré superlattices ($D_{moiré}$ ~7.7 nm [5]) in cleaved highly oriented pyrolytic graphite (HOPG). Comparable moiré superlattices were further reported in 2012 by Brihuega et al. in few-layers graphene ($D_{moiré}$ ~1.5 nm, ~ 2.2 nm, ~ 4.1 nm and 10.1 nm [10]). By applying the equation $a/2D=\sin(\theta/2)$ [7-10] where a is the basal lattice constant of HOPG (~ 0.247 nm), D is the period of the moiré pattern and θ is the rotational angle, the following rotational angles θ_{rot} ~ 1.8º [5] and ~ 9.6º, 6.4º, 3.5º, 1.4º [10] were identified on the basis of the scanning tunnelling microscopy acquisitions (STM) [5, 10]. Comparable hexagonal moiré superlattices were reported in HOPG also by Kuwabara et al. in 1990 (D ~ 7.7 nm, θ_{rot} ~ 1.8º) [7], by Patil et al. in 2017 (D ~ 6.8 nm, ~ 8.4 nm, ~ 9.2 nm corresponding to θ_{rot} ~ 2.1º, 1.7º and 1.5º) [8] and by Flores et al. in 2013 (D ~ 4.8 nm, ~ 1.5 nm corresponding to θ_{rot} ~ 2.9º, 9.4º) [9]. VHs singularities were further reported at room-temperature by Zhang et al. in exfoliated HOPG [11].

Interestingly, a model of quasi-two-dimensional (2D) interfaces, namely the Burgers–Bragg–Read–Shockley (BBRS) dislocation model [12], was proposed by Esquinazi et al. in order to explain the origin of unusual superconductive-like effects observed at high temperature in HOPG [13-17].

Also, anomalous negative thermal expansion and saturation effects at low temperature have been recently reported by our group in this class of materials by employing temperature dependent X-ray diffraction (T-XRD) [24]. Being interested in

investigating further the structural properties of those HOPG samples exhibiting such an unusual thermal expansion effect, we have performed a novel investigation by employing STM, STS, transmission electron microscopy (TEM) and T-XRD.

By employing STS, we investigated the local density of states (LDOS) properties of sample-areas exhibiting moiré superlattices, identified by STM on the surface of as purchased-HOPG; this method allowed for the observation of vHs in those locally twisted sample-regions. Precisely LDOS analyses were performed on moiré superlattices with periodicity D of ~ 4 nm (θ_{rot} of ~ 3.6º), ~ 2 nm (θ_{rot} of ~ 7.08º) and ~ 0.5 nm (θ_{rot} of ~ 28.6º). The vHs-separation parameter was investigated for a fixed rotational angle (θ_{rot} of ~ 3.6º) which was identified in multiple surface areas of the same HOPG sample. Investigation of the spatial distributions of the moiré superlattices within the HOPG sublattices was further performed by employing TEM on exfoliated lamellae. These measurements allowed the frequent identification of other hexagonal periodicities D of ~ 13.87 nm (θ_{rot} of ~ 1.02º), ~ 13.0 nm (θ_{rot} of ~ 1.09º), ~ 12.65 nm (θ_{rot} of ~ 1.12º) and ~ 2.03 nm (θ_{rot} of ~ 7.0º). These observations were further supported by additional LDOS spectra acquired from moiré-superlattice-periodicities D ~8 nm (θ_{rot} ~1.8º). In the latter, unusual presence of four vHs peaks highlighted existence of multiple rotational effects between internal sublattices. An HOPG sample with mosaic-angle and grade (grade B) identical to those analysed with STM/STS (grade A, B) and exhibiting negative thermal expansion was further investigated by T-XRD from 12K to 298K. While these data were previously reported in ref.24, here we present an extended analysis on peak-features and 2θ-regions not previously reported. In particular, we highlight the presence of two unknown peak features for $2\theta \sim 21^{\circ}$ and $\sim 43^{\circ}$ and their temperature dependent characteristics. Also, we evidence the observation of a not-previously reported exfoliation-induced distortion of the hexagonal moiré superlattices in some of the lamellae. We attribute this phenomenon to an enhanced topological disorder created by the directional shear forces which are present during the tape-exfoliation process. Zero field cooled (ZFC) and field cooled (FC) magnetic measurements acquired with superconducting quantum interference device (SQUID) magnetometry

from those samples, revealed a not previously reported anisotropic ferromagnetic behaviour.

By applying the mFC-mZFC subtraction method, a transition could be detected at ~ 50K. The significant anisotropic trend of the acquired signals, evidences additional magnetic components (for lamella-layers-orientation perpendicular to the applied magnetic field) possibly arising from the locally twisted sublattices exhibiting moiré superlattices. The possible presence of variable periodic stacking between twisted sublattices may play also a significant role in inducing shifts in the expected values of the magic angle required for observation of orbital ferromagnetic ordering (θ_{rot} ~ 1.2º [27]) and exotic ferromagnetism (θ_{rot} ~ 1.8º [4]).

2 Experimental

HOPG samples of grade A,B with dimensions of 5 x 5 x 1 mm and mosaic angles of 0.5°, 0.8° ± 0.2° were purchased from XFNANO, INC China. STM and STS measurements were performed on the surface of the as purchased HOPG sample by employing a USM 1300-He3 instrument at 77K. The lamellae used for the comparative investigation of the spatial moiré distribution were prepared through tape-exfoliation (following the method reported in ref. [**20**]) and analysed by TEM and SQUID. TEM images were acquired with a 200 kV American FEI Tecnai G2F20. SQUID, ZFC and FC magnetic signals were acquired by employing a Quantum design instrument from 2K to 300K.

T-XRD measurements were performed on HOPG samples with identical grade (grade B) to those analysed with STM/S by employing a PANalytical Empyrean powder X-ray diffractometer (Cu K-α_1, λ =0.15406 nm), equipped with a primary Johansson monochromator, an Oxford Cryosystems PheniX cryostat operating under vacuum below 10^{-2} Pa, and a X'celerator linear detector, from 12 K to 298 K (12 K, 20 K, 30 K, 40 K, 50 K, 60 K, 70 K, 80 K , 90 K, 100 K, 120 K, 140 K, 160 K, 180 K, 200 K, 220 K, 240 K, 260 K, 280 K and 298 K).

3 Results and Discussion

Hexagonal moiré superlattices were identified in locally twisted surficial-areas of HOPG (as purchased) by STM, as shown in Fig.1. Locally twisted surficial areas revealed periodicities D of ~ 0.5 nm (θ_{rot} of ~ 28.6º in Fig.1A-D), ~ 2 nm (θ_{rot} of ~ 7.08º in Fig.1G,H) and ~ 4 nm (θ_{rot} of ~ 3.6º see Fig.2A-C). LDOS spectra acquired from the areas exhibiting θ_{rot} of ~ 28.6º and θ_{rot} of ~ 7.08º are shown in Fig.1E,F and Fig.1I. Broad peak-features (see Fig.1E,F and Fig.1I) corresponding to the vHs were detected within the first two types of moiré areas (see Fig.1A-D, Fig.1G-H), instead sharp peaks in the LDOS spectra were acquired from the moiré areas with D ~ 4 nm (θ_{rot} of ~ 3.6º, Fig.2A-C) as shown in Fig.2D-F. The variable intensity and especially the weaker vHs contribution observed for θ_{rot} of ~ 28.6º can be ascribed to the larger value of θ_{rot} [6, 10, 21].

The scans 1-5 in Fig.2D-F represent the spectra acquired from 5 different moiré areas which exhibited a comparable θ_{rot} of ~ 3.6º. It is evident the appearance of sharp peaks corresponding to the vHs.

Considering the dimensions of the analysed HOPG are ~ 5 mm x ~ 5 mm x 1 mm, it is important to comment also on the possible effects of the multi-layered nature of the sample on the as-measured position of the vHs in the LDOS spectra. Interestingly significant shifts in the peak-position of the vHs were found in areas with comparable θ_{rot} of ~ 3.6º. Specifically, the LDOS spectra acquired from 5 different areas exhibiting moiré superlattices with D ~ 4 nm are shown with higher detail in Fig.3A-E. A clear shift in the position of the vHs could be detected by calculating the vHs-separation, as shown in Fig.3F. Interestingly, a previous report by Brihuega et al. [10] highlighted an important dependence of the singularities-peak-position on the local interlayer distances between graphene layers and therefore on the values of the interlayer coupling parameter (interlayer potential) [10].

In addition to this interpretation, the thickness (i.e. number of periodically-twisted layers) of the analysed moiré areas may influence the outcome of the acquired LDOS spectra [10,19]. This particular aspect was computed in a recent work by Khalaf et al. [19], by considering a model of alternating-twist in multilayer graphene. It was shown that by considering n_e sequences of magic angles and multiplying the twisted bilayer graphene magic angles by 2cos ($\pi * k/ n+1$) (with k = 1,…..,n_e), significant shifts in the magic angle values could be found, obtaining $\sqrt{2}$ for n = 3 and 2 for $n \rightarrow \infty$.

In an attempt to gain additional insights on the spatial distribution of the hexagonal moiré superlattices within the sublattices of the HOPG sample, additional investigation was performed in lamellae exfoliated from inner regions. By employing TEM, other locally twisted areas exhibiting hexagonal moiré superlattices could be frequently identified, as shown in Fig.4A-H. Hexagonal moiré superlattices (see Fig.4A-C and magenta circles in Fig.4B) with periodicities of ~ 13.87 nm in Fig.4D (θ_{rot} of ~ 1.02º), ~ 13.0 nm in Fig.4G,H (θ_{rot} of ~ 1.09º), ~ 12.65 nm in Fig.4E,F (θ_{rot} of ~ 1.12º) and ~ 2.03 nm in Fig.4E,F (θ_{rot} of ~ 7.0º) were found. The observed moiré periodicities resemble those reported by Li et al. [5], Kuwabara et al. [7], Patil et al. [8] and Brihuega et al. [10]. In particular in Fig.4G-H note the sudden disappearance of the hexagonal superlattice, which highlights the locality of the twisting effect (i.e. locally twisted areas, or stacking-faults) in an otherwise Bernal system.

Additional analyses were then sought by STM on comparable locally twisted areas exhibiting multiple rotational effects, in analogy with those observed in Fig.4E,F by TEM. These analyses are shown in Fig.5. The STM measurements revealed also in this case the presence of hexagonal moiré superlattices with periods D of ~ 8 nm (θ_{rot} of ~ 1.8º) as shown in Fig.5A,B. Average LDOS spectra were acquired on the blue dashed lines, as shown in Fig.5C,D. Note the appearance of 4 sharp peaks corresponding to the vHs. The presence of peaks 1 and 4 in proximity of the vHs peaks expected for θ_{rot} of ~ 1.8º (peaks 2 and 3), appears to be an indicator of multiple rotational effects possibly arising from other twisted internal sublattices, in analogy to the case observed in Fig.4E,F.

Extended analyses were then performed on the T-XRD dataset acquired from an HOPG sample with grade B from 12K to 298K, identical to those analysed with STM/STS (grade A,B) and exhibiting negative thermal expansion [24]. Unknown peak-features (not reported in ref.24) were found at $2\theta \sim 21^{\circ}$ (Fig.6A-C) and $\sim 43^{\circ}$ (Fig.6A, D). Interestingly, the plots presented in Fig.6E, F (indicating the T-dependent variation of the 2θ peak position) revealed a peak shift analogous to that of the 002 reflection in the T-range from T~160K to T~298K. Deviation from the T-dependent trend reported in ref.24 for the 002 peak-reflection was then found below T~160K. This is shown in Fig.6E and ESI Fig.S1,2 for $2\theta \sim 21^{\circ}$ and in Fig.6F for $2\theta \sim 43^{\circ}$. This observation differs from the trend reported in ref. [24], where an anomalous negative-thermal-expansion effect was found from ~12 K to ~50 K. This result may possibly represent an indicator of multiple graphitic phases (i.e. coexistence of Bernal ordering and locally rotated sublattices as shown in Figs.1-5) contributing to the thermal expansion process and implies that the interlayer potential parameter may also vary with the temperature.

Further TEM-analyses were then performed in an attempt to investigate possible superlattices-modification induced by the shear forces involved in the exfoliation process. As shown in Fig.7A-D these measurements allowed the identification of a not-previously reported distortion of the hexagonal moiré superlattices in some of the exfoliated lamellae; this effect appears to be a possible indicator of topological disorder induced by the exfoliation process (see also Fig.7B-D).

Further characterization of this latter type of samples was sought by employing SQUID magnetometry. The ZFC and FC magnetic signals acquired from the exfoliated lamella are shown in Fig.7E,F with sample-layers-orientation parallel (Fig.7E) and perpendicular (Fig.7F) to the applied field.

According to the percolative theory reported in ref. 22, uncorrelated ferromagnetic clusters can be observed below a certain temperature T^{*} in presence of topological disorder, leading to finite values of M_s(temperature T, applied field H), M_{rem}(T,H), and ΔM(T,H) [22]. As the temperature decreases, ferromagnetic correlations develop on a larger scale, and eventually a long-range ferromagnetic order emerges. The

ZFC-FC magnetization irreversibility shown in Fig.7E-G evidences an enlargement of pre-existing ferromagnetic clusters below 50K. It is noticeable the presence of an unusual anisotropic behaviour in the value of the magnetic moment measured in the ZFC and FC curves (in Fig.7E,F) [22-23,25]. By subtracting the magnetic moment of the ZFC curve to the magnetic moment of the FC curve (i.e. mFC – mZFC [22,23,25]), a transition common to both the sample orientations could be detected at ~ 50K in Fig.7G. It is however important to notice the significant anisotropic behaviour, evidenced by the red and black subtraction-plots (in Fig.7G), which seems indicative of additional magnetic components arising at low temperature.

The observed enhanced magnetic contribution (for sample-layers-orientation perpendicular to the applied field) may be attributable to the locally twisted sublattices shown in Figs.1,2,4,5. As evidenced by the STS measurements in Fig.3, the possible presence of variable periodic stacking between twisted sublattices may play also a significant role in inducing shifts in the expected values of the magic angle required for observation of orbital ferromagnetic ordering (expected value for twisted bilayer graphene, TBG θ_{rot} ~ 1.2º [27]) or exotic ferromagnetism (expected value for TBG θ_{rot} ~ 1.8º [4]) and for superconductivity (expected value for TBG θ_{rot} ~ 1.09º [1]).

Together with these observations, it is also important to mention that an enhancement in the relative abundance of rhombohedral phases (ABCA stacking) can occur as a consequence of the exfoliation process; this effect has been recently shown in presence of shear forces, during exfoliation of multilayer graphene [28-30].

Further, a recent work by Kerelsky et al. [31] has demonstrated that micrometre-scale regions of uniform rhombohedral (four-layer, ABCA) graphene can be obtained under certain conditions of small twist-angles (<0.1°) between two Bernal-bilayers. Existence of a ferrimagnetic state within the topmost layer and of an antiferromagnetic ordering across the topmost and bottommost layer was further reported in conditions of zero displacement-field [31]. On the basis of these reports, we can not exclude the presence of possible weak contributions arising from

rhombohedral impurities. This aspect will be carefully investigated in our future work.

4 Conclusion

In conclusion we reported a novel investigation of the electronic and magnetic properties of HOPG samples exhibiting negative thermal expansion properties, by employing STM, STS, TEM, T-XRD and SQUID. We demonstrated presence of vHs singularities identified in the LDOS spectra acquired from moiré-superlattices with periodicity D ~ 4 nm (θ_{rot} of ~ 3.6º), ~ 2 nm (θ_{rot} of ~ 7.08º) and ~ 0.5 nm (θ_{rot} of ~ 28.6º). A variation in the vHs-separation was further found in STS measurements performed in multiple-moiré-areas exhibiting comparable θ_{rot} ~ 3.6º. The variation of this parameter was attributed to 1) local changes in the interlayer coupling parameter and 2) local variation of the thickness (i.e. periodic stacking of twisted layers) of the moiré areas and 3) possible variation of the twisting angle in the internal sublattices. The spatial-sublattice-distribution of the moiré-superlattices was further investigated by TEM of exfoliated lamellae and allowed the identification of periodicities D of ~ 13.87 nm (θ_{rot} ~1.02º), ~ 13.0 nm (θ_{rot} ~1.09º), ~ 12.65 nm (θ_{rot} ~1.12º) and ~ 2.03 nm (θ_{rot} ~ 7.0º). T-XRD revealed the presence of unknown peak features exhibiting significant T-induced shifts towards lower 2θ values as the temperature increased from ~160K to ~298K, together with an unusual low-temperature saturation effect.

ZFC and FC magnetic signals revealed a significant anisotropic-behaviour in those exfoliated lamellae exhibiting an enhanced topological disorder and an unusual exfoliation-induced distortion of the moiré superlattices. By subtracting the magnetic moment of the ZFC curve to the magnetic moment of the FC curve, a transition common to both the sample orientations could be detected at ~ 50K. We evidenced the presence of a significant anisotropic behaviour of the acquired signals (for lamella-layers-orientation perpendicular to the applied magnetic field). This seems indicative of additional magnetic components present in the sample. Further work is needed to clarify possible influences arising from locally twisted sublattices with θ_{rot}

~ 1.2º and θ_{rot} ~ 1.8º and/or from rhombohedral impurities produced by the exfoliation process.

Acknowledgments

Prof. Filippo Boi acknowledges research support from NSFC fund 11950410752 and Sichuan Province fund 2019YFH0080. Prof. Shanling Wang acknowledges research support from laboratory and equipment management funding SCU201208 (Sichuan University).

Declaration of interests

The authors declare that they have no known competing financial interests or personal relationships that could have appeared to influence the work reported in this paper.

References

[1] Cao Y., Fatemi V., Fang S., Watanabe K., Taniguchi T., Kaxiras E. and Jarillo-Herrero P. Unconventional superconductivity in magic-angle graphene superlattices. Nature 2018; 556: 43–50.

[2] Cao Y., Fatemi V., Demir A., Fang S., Tomarken S. L., Luo J. Y., Sanchez-Yamagishi J. D., Watanabe K., Taniguchi T., Kaxiras E., Ashoori R. C. and Jarillo-Herrero P. Nature 2018; 556: 80–84.

[3] Arora H.S., Polski R., Zhang Y. et al. Superconductivity in metallic twisted bilayer graphene stabilized by WSe2. Nature 2020; 583: 379–384.

[4] Seo K., Kotov V. N. and Uchoa B. Ferromagnetic Mott state in Twisted Graphene Bilayers at the Magic Angle. Phys. Rev. Lett. 2019; 122: 246402

[5] Li G., Luican A., Lopes dos Santos J. M. B., Castro Neto A. H., Reina A., Kong J. and Andrei E. Y. Observation of Van Hove singularities in twisted graphene layers. Nature Physics 2010; 6:109–113.

[6] Luican A., Li G., Reina A., Kong J., Nair R. R., Novoselov K. S., Geim A. K., and Andrei E.Y. Single-Layer Behavior and Its Breakdown in Twisted Graphene Layers. Physical Review Letters 2011; 106: 126802.

[7] Kuwabara M., Clarke D. R., and Smith D. A. Anomalous superperiodicity in scanning tunneling microscope images of graphite. Appl. Phys. Lett. 1990; 56: 2396.

[8] Patil S., Kolekar S., Deshpande A. Revisiting HOPG superlattices: Structure and conductance properties. Surface Science 2017; 658: 55–60.

[9] Flores M., Cisternas E., Correa J., and Vargas P. Moiré patterns on STM images of graphite induced by rotations of surface and subsurface layers. Chem. Phys. 2013; 423: 49.

[10] Brihuega I., Mallet P., González-Herrero H., de Laissardière G. T., Ugeda M. M., Magaud L., Gómez-Rodríguez J. M., Ynduráin F., and Veuillen J.-Y. Unraveling the Intrinsic and Robust Nature of van Hove Singularities in Twisted Bilayer Graphene by Scanning Tunneling Microscopy and Theoretical Analysis. Phys. Rev. Lett. 2012; 109: 196802.

[11] Zhang X., Luo H. Scanning tunneling spectroscopy studies of angle-dependent van Hove singularities on twisted graphite surface layer. Applied Physics Letters 2013; 103: 231602.
[12] Esquinazi P., Heikkilä T. T., Lysogorskiy Y. V., Tayurskii D. A., and Volovik G. E. On the Superconductivity of Graphite Interfaces. JETP Letters 2014; 100: 336–339.
[13] Brandt N.B., Kotosonov A.S., Kuvshinnikov S.V., Semenov M.V. The possibility of increasing diamagnetic susceptibility of pyrocarbon. JETP letter 1979; 29: 720-722.
[14] Kopelevich Y., Lemanov V. V., Moehlecke S. and Torres J. H. S. Landau level quantization and possible superconducting instabilities in highly oriented pyrolytic graphite. Physics of the Solid State 2002; 41: 1959-1962.
[15] Kopelevich Y., Esquinazi P., Torres J. H. S., Moehlecke S. Ferromagnetic- and Superconducting-Like Behavior of Graphite. Journal of Low Temperature Physics 2000; 119: 691-702.
[16] Scheike T., Esquinazi P., Setzer A., and Böhlmann W. Granular superconductivity at room temperature in bulk highly oriented pyrolytic graphite samples. Carbon 2013; 59:140.
[17] Volovik G. E. Graphite, Graphene, and the Flat Band Superconductivity. JETP Letters 2018; 107: 516-517
[18] Ramnani P., Neupane M. R., Ge S., Balandin A. A., Lake R. K., Mulchandani A. Raman spectra of twisted CVD bilayer graphene. Carbon 2017; 123: 302-306.
[19] Khalaf E., Kruchkov A. J., Tarnopolsky G., and Vishwanath A. Magic angle hierarchy in twisted graphene multilayers. Phys. Rev. B 2019; 100: 085109.
[20] Boi F. S., Shuai G., Wen J. and Wang S. Unusual moiré superlattices in exfoliated μm-thin HOPG lamellae: An angular-diffraction study. Diamond and Related Materials 2020; 108: 107920.
[21] Peng H., Schröter N. B. M., Yin J., Wang H., Chung T.-F., Yang H., Ekahana S., Liu Z., Jiang J., Yang L., Zhang T., Chen C., Ni H., Barinov A., Chen Y. P., Liu Z., Peng H. and Chen Y. Substrate Doping Effect and Unusually Large Angle van Hove Singularity Evolution in Twisted Bi- and Multilayer Graphene. Adv. Mater. 2017; 29: 1606741.
[22] Kopelevich Y., da Silva R. R., Torres J. H. S., Penicaud A., and Kyotani T. Local ferromagnetism in microporous carbon with the structural regularity of zeolite Y. Phys. Rev. B 2003; 68: 092408.
[23] Theodoropoulou N., Hebard A. F., Overberg M. E., Abernathy C. R., Pearton S. J., Chu S. N. G., and Wilson R. G. Unconventional Carrier-Mediated Ferromagnetism above Room Temperature in Ion-Implanted (Ga, Mn)P:C. Phys. Rev. Lett. 2002; 89: 107203.
[24] Taallah A., Shuai G., Odunmbaku O., Corrias A. and Boi F. S. Anomalous low-temperature saturation effects and negative thermal expansion in the c-axis of highly oriented pyrolytic graphite at the magic angle. Materials Research Express 2020; 7: 015614
[25] Boi F. S., Gao S., He Y., and Wang S. Percolative magnetic correlation and competing-antiferromagnetism in highly oriented pyrolytic graphite with hexagonal moiré superlattices at the magic-angle. Materials Research Express 2020; 7: 125602.
[26] Boi F. S., Gao S., Lei L., Taallah A. and Wang S. Annihilation of percolative correlation signals in sulfur doped highly oriented pyrolytic graphite with hexagonal moiré superlattices. Diamond and Related Materials 2021; 111: 108186
[27] Sharpe, A. L.; Fox, E. J.; Barnard, A. W.; Finney, J. ; Watanabe, K. ; Taniguchi, T. ; Kastner, M. A. ; Goldhaber-Gordon, D. Emergent ferromagnetism near three-quarters filling

in twisted bilayer graphene. Science 2019; 365: 605-608
[28] Yang Y., Zou Y.-C., Woods C. R., Shi Y., Yin J., Xu S., Ozdemir S., Taniguchi T., Watanabe K., Geim A. K., Novoselov A. K., Haigh S. J., and Mishchenko A. Stacking Order in Graphite Films Controlled by van der Waals Technology. Nano Lett. 2019; 19: 8526−8532
[29] Henni Y., Collado H. P. O., Nogajewski K., Molas M. R., Usaj G., Balseiro C. A., Orlita M., Potemski M. and Faugeras C. Rhombohedral Multilayer Graphene: A Magneto-Raman Scattering Study, Nano Lett. 2016; 16: 3710−3716
[30] Shi Y., Xu S., Yang Y., Slizovskiy S., Morozov S. V., Son S.-K., Ozdemir S., Mullan C., Barrier J., Yin J., Berdyugin A. I., Piot B. A., Taniguchi T., Watanabe K., Fal'ko V. I., Novoselov K. S., Geim A. K. and Mishchenko A. Electronic phase separation in multilayer rhombohedral graphite. Nature 2020; 584: 210–214.
[31] Kerelsky A., Verdú C. R., Xian L., Kennes D. M., Halbertal D., Finney N., Song L., Turkel S., Wang L., Watanabe K., Taniguchi T., Hone J., Dean C., Basov D. N., Rubio A., and Pasupathy A. N. Moiréless correlations in ABCA graphene. PNAS 2021;118: e2017366118.

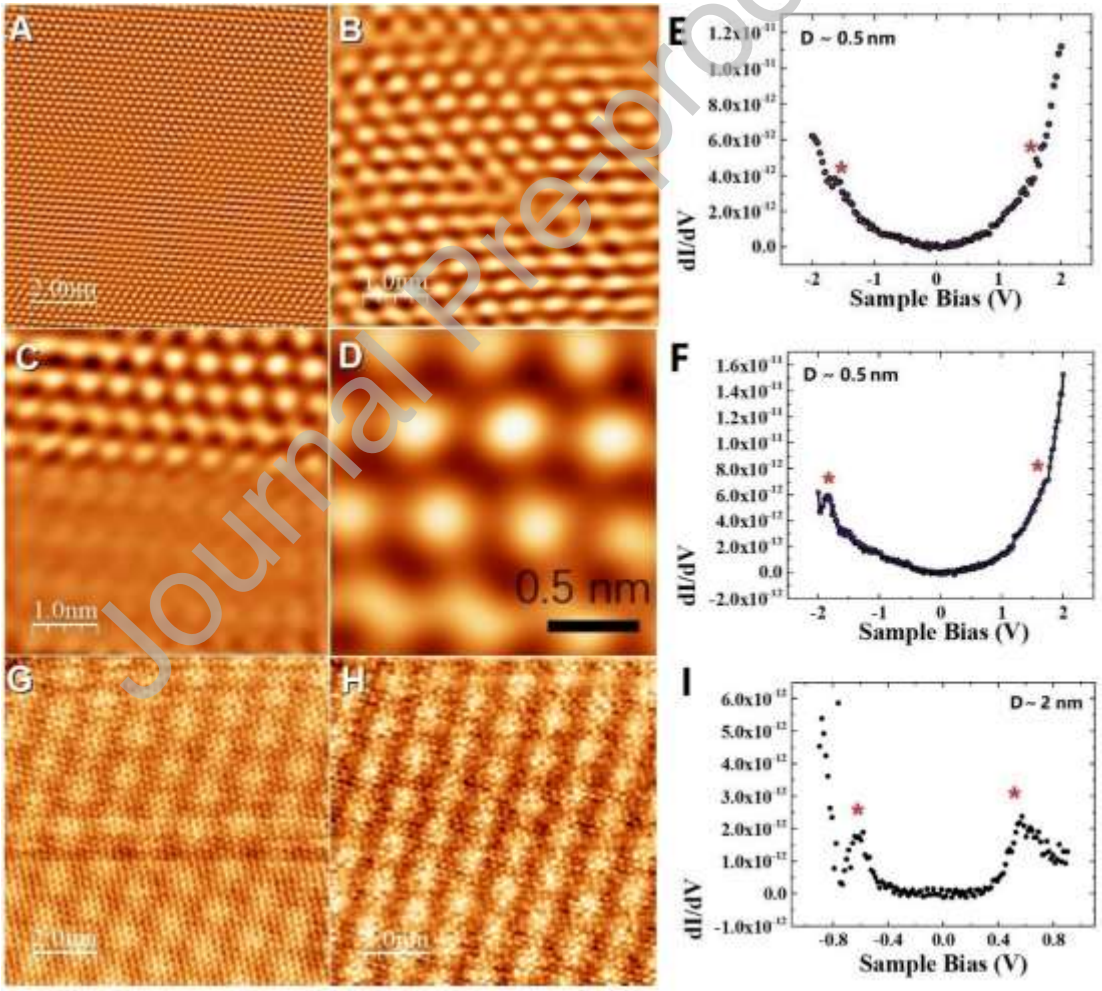

Figure 1: STM measurements performed on the surface of as purchased HOPG sample. Presence of hexagonal moiré superlattices in locally twisted surficial-areas is shown in Fig.1A-D and Fig.1G. The locally twisted areas were found to exhibit moiré superlattices with periods D of ~ 0.5 nm (θ_{rot} of ~ 28.6º in Fig.1A-D) and D ~ 2 nm

(θ_{rot} of ~ 7.08º in Fig.1G, H). LDOS spectra acquired from the areas exhibiting θ_{rot} of
~28.6º are shown in Fig.1E,F while that acquired from the area exhibiting θ_{rot} of ~ 7.08º is shown in Fig.1I. Broad peaks corresponding to the vHs were detected in the LDOS acquired from both the moiré areas. In particular, note the weaker intensity of the vHs observed for θ_{rot} of ~ 28.6º, which can be attributed to the much larger value of θ_{rot} [6,10,21].

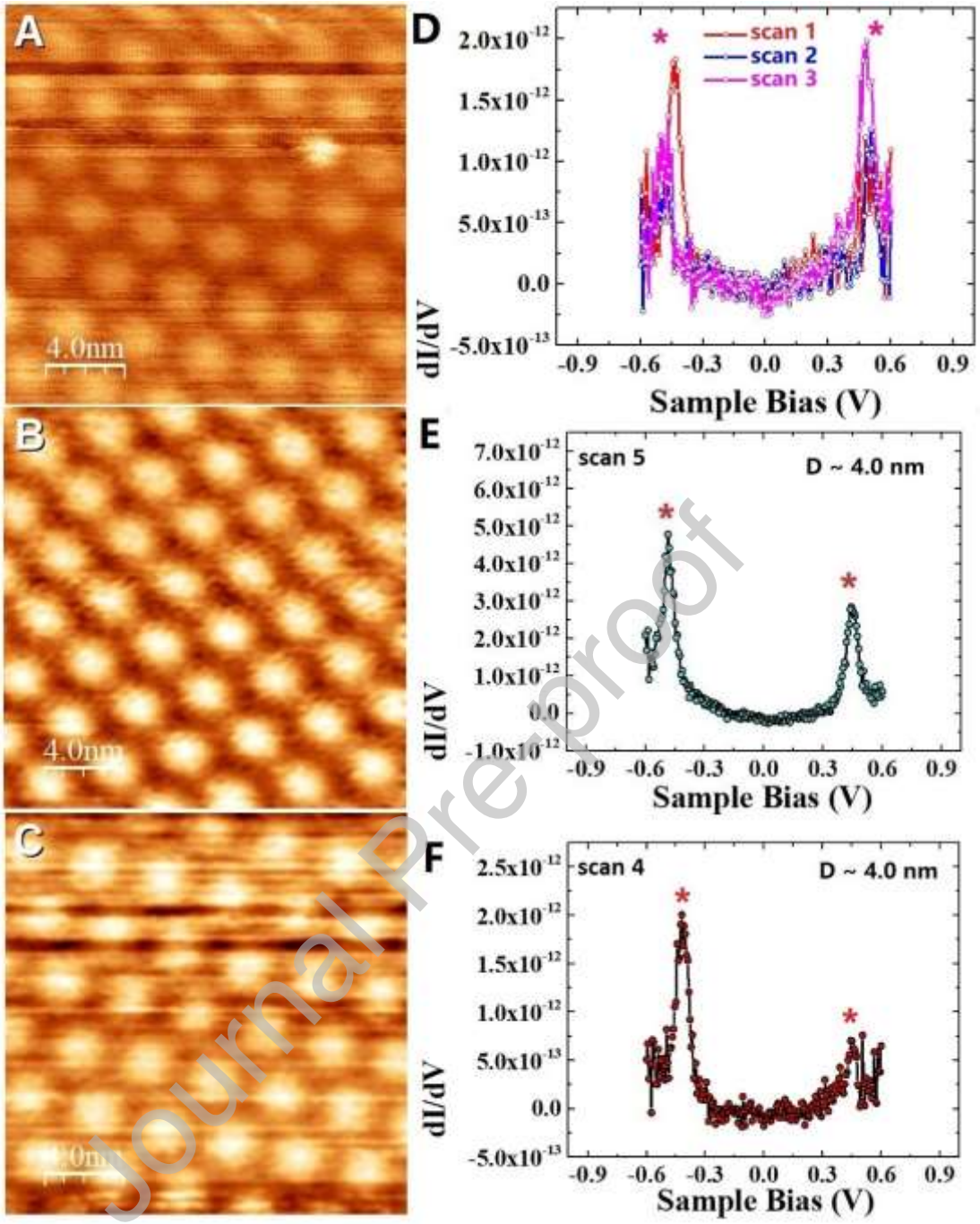

Figure 2: STM measurements revealing presence of hexagonal moiré superlattices in locally twisted surficial-areas of HOPG (Fig.2A-C). These locally twisted areas were found to exhibit moiré superlattices with periods D of ~ 4 nm (θ_{rot} of ~ 3.6º in Fig.2A-C). LDOS spectra acquired from these areas (θ_{rot} of ~ 3.6º) are shown in Fig.2D-F. Note the appearance of sharp peaks corresponding to the vHs.

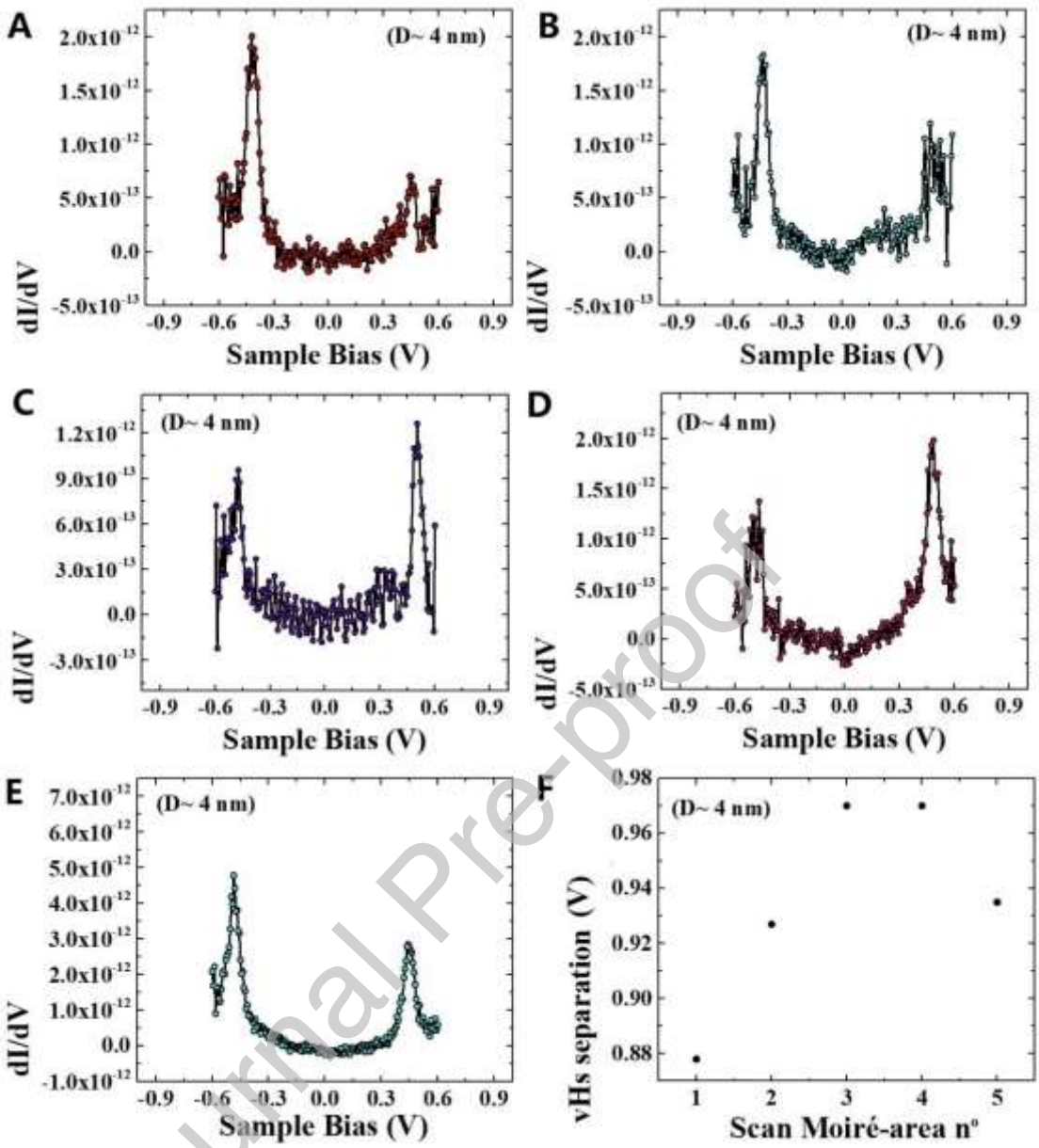

Figure 3: In Fig.3A-E, detailed LDOS spectra acquired from the locally twisted areas exhibiting moiré superlattices with period D ~ 4 nm, corresponding to θ_{rot} of ~ 3.6º. Sharp peaks corresponding to the vHs were found. In Fig.3F the extracted vHs separation parameter is plotted for all the 5 analyses areas. Note the variation in the separation values, which possibly arises from local changes of the interlayer distances between graphene layers and/or from local variation in the thickness (i.e. periodic stacking of twisted layers) of the moiré areas.

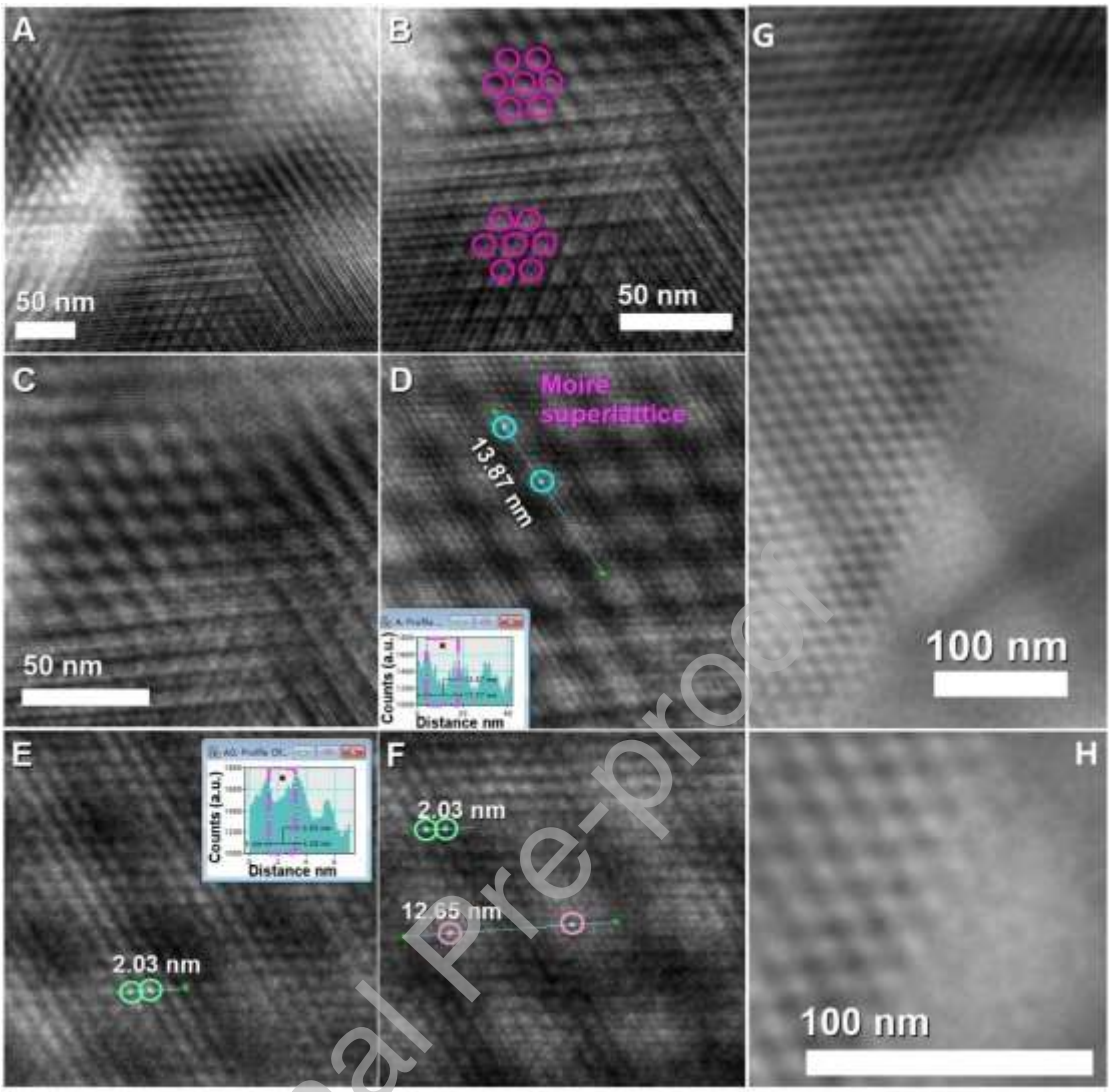

Figure 4: TEM analyses performed on lamellae exfoliated from internal regions (sublattices) of HOPG. Locally twisted areas exhibiting hexagonal moiré superlattices could be identified, as shown in Fig.4A-H (see magenta circles in Fig.4B). Superlattice periodicities D of ~ 13.87 nm in Fig.4D (θ_{rot} of ~ 1.02º), ~ 13.0 nm in Fig.4G,H (θ_{rot} of ~ 1.09º), ~ 12.65 nm in Fig.4E,F (θ_{rot} of ~ 1.12º) and ~ 2.03 nm in Fig.4E,F (θ_{rot} of ~ 7.0º) were found. In Fig.4G-H note the sudden disappearance of the D ~ 13.0 nm period. This observation highlights the locality of the twisting effect in the analysed lamella. Particularly in F, note the presence of multiple periodicities, indicative of multiple rotated interfaces coexisting in the same sublattices. Note that the average dimensions of the areas exhibiting the moiré superlattices were ~ 1 μm x 1μm, as shown in the schematic in ESI.

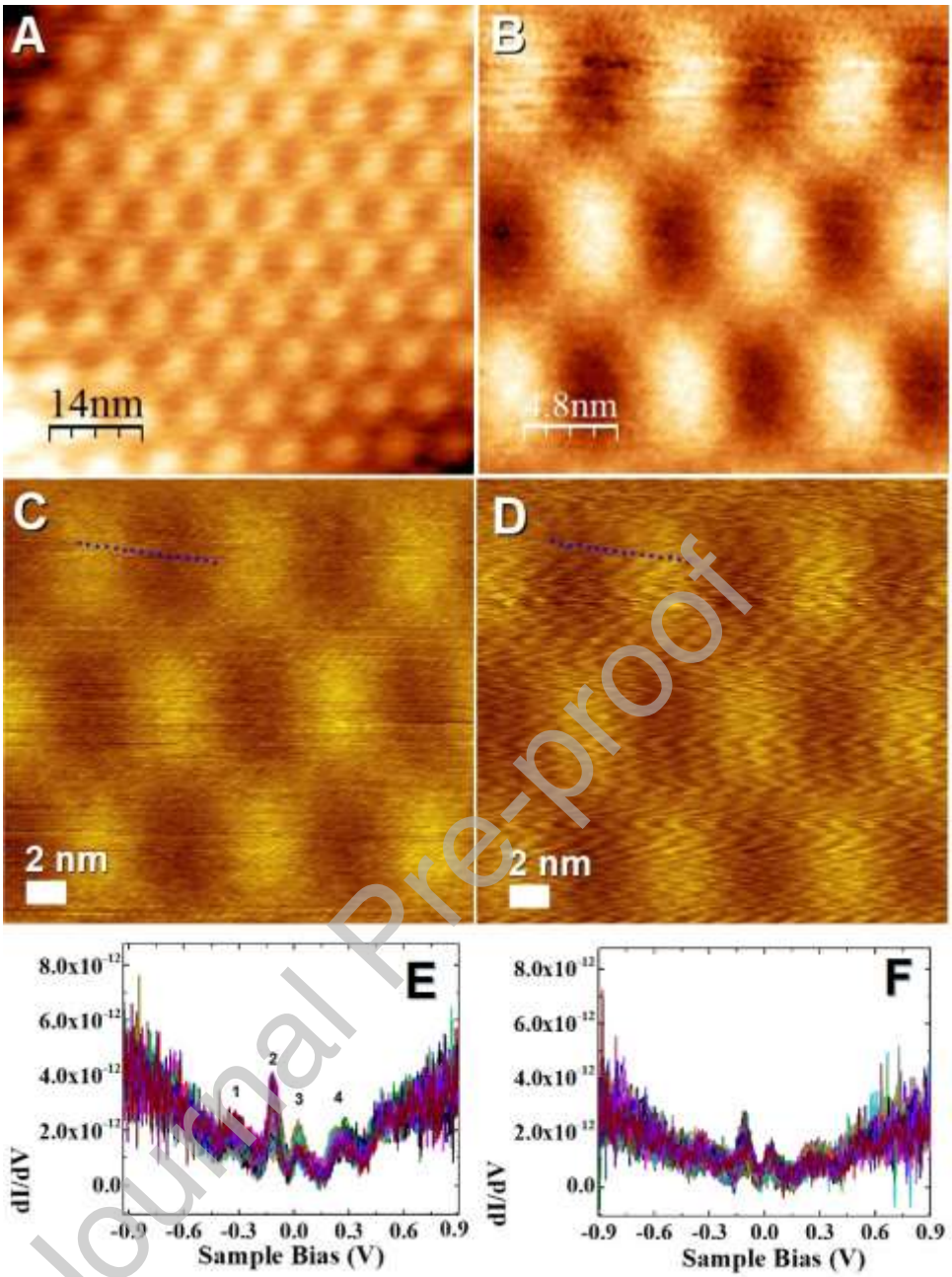

Figure 5: STM measurements revealing the presence of hexagonal moiré superlattices in other locally twisted surficial-areas of HOPG, in agreement with the TEM measurement in Fig.4. These locally twisted areas were found to exhibit moiré superlattices with periods D of ~ 8 nm (θ_{rot} of ~ 1.8º) as shown in A,B. LDOS spectra (E,F) were acquired through lines-acquisition from the areas shown in C,D respectively. Note the unusual appearance of 4 peaks corresponding to the vHs. Particularly, appearance of the peaks 1 and 4 seems to be an indicator of multiple rotational effects of internal sublattices, similarly to the case observed in Fig.4E,F. Instead, the peaks 2,3 are representative of hexagonal moiré superlattices with D ~ 8nm, corresponding to θ_{rot} ~ 1.8º

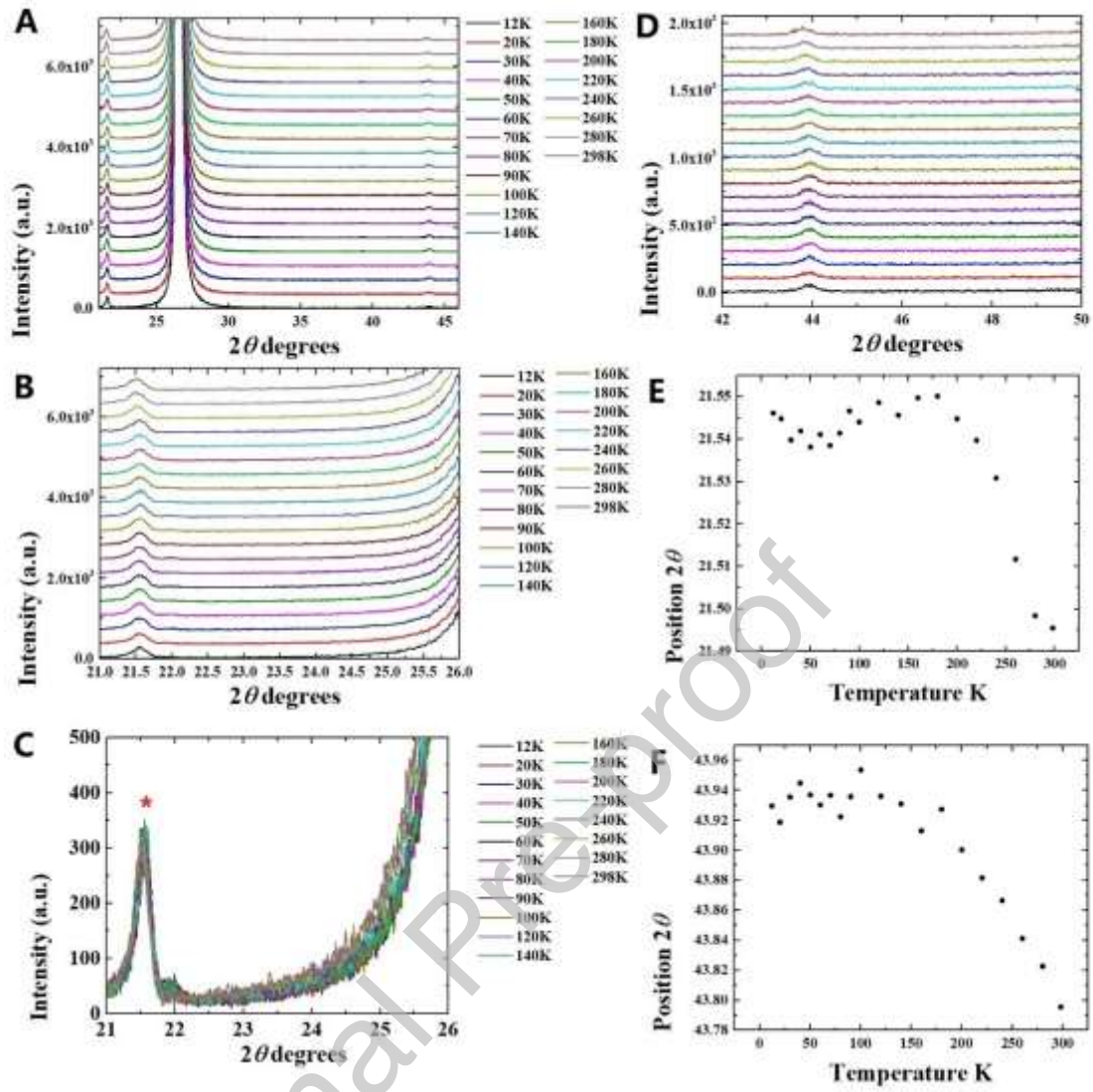

Figure 6: Extended analyses performed on the T-XRD dataset acquired from an HOPG sample with grade B and exhibiting negative thermal expansion [24]. Unknown peak-features (not presented in ref.24) were found at $2\theta \sim 21^{\circ}$ (Fig.6A-C) and $\sim 43^{\circ}$ (Fig.6A,D). Interestingly, the plots presented in Fig.6E,F (indicating the T-dependent variation of the 2θ peak position) revealed a peak shift analogous to that of the 002 reflection in the T-range from T~160K to T~298K. Deviation from the trend reported in ref.24 was then found below T~160K. Interestingly the shift in the peaks observed for $2\theta \sim 21^{\circ}$ (Fig.6E) and $\sim 43^{\circ}$ (Fig.6F) was found to approximately saturate in the T-range from ~ 160K to 12K. This observation differs from the trend observed in the 002 peak, where an anomalous negative-thermal-expansion effect was found from ~12 K to ~50 K.

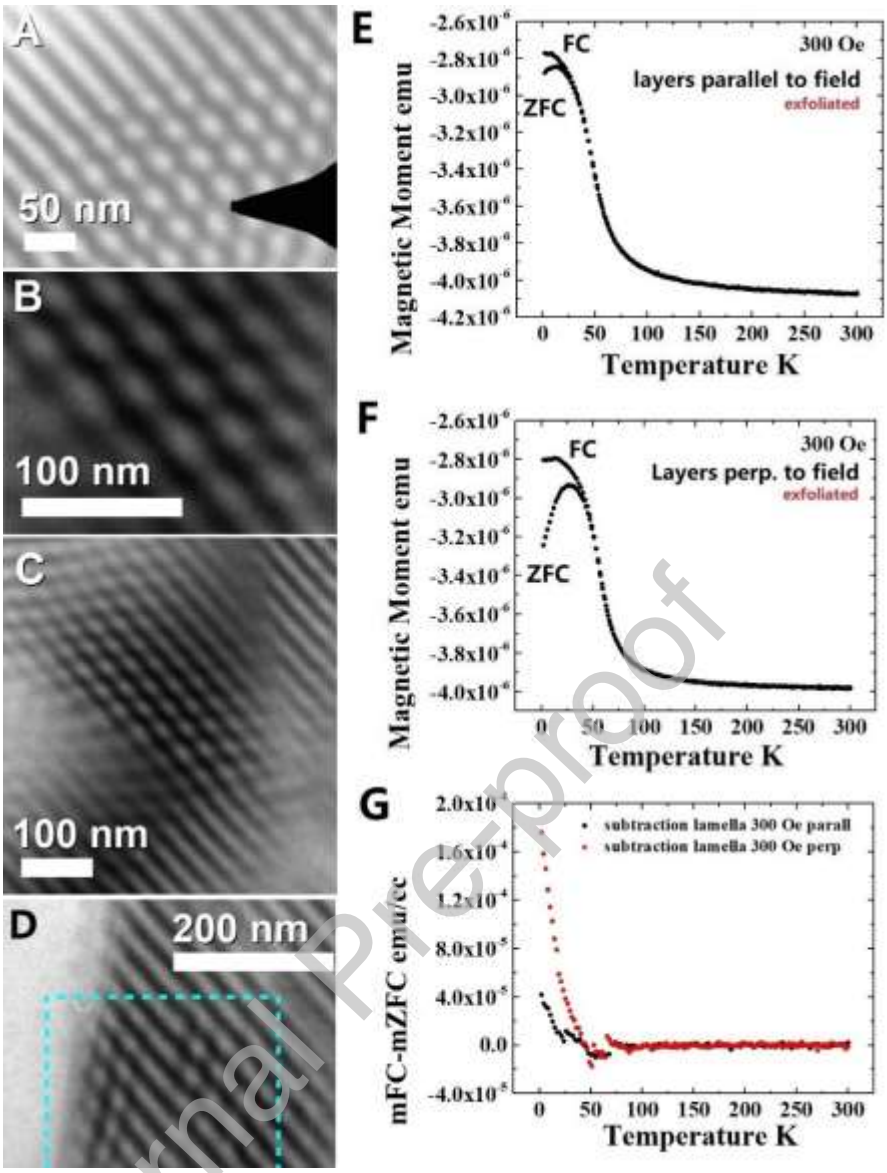

Figure 7: TEM micrographs in Fig.7A-D, highlighting the presence of not-previously reported distortion of the hexagonal moiré superlattices in some areas of the exfoliated lamella; this is shown also in proximity of the lamellae edges (Fig.7D) by the dashed area. This effect can be identified as a possible indicator of topological disorder induced by the directional shear forces involved in the exfoliation process. In Fig.7E-G ZFC and FC magnetic signals and mFC-mZFC subtraction acquired from an exfoliated lamella exhibiting the enhanced topologically disordered areas. By subtracting the magnetic moment of the ZFC curve to the magnetic moment of the FC curve, a transition common to both the sample orientations could be detected at ~ 50K. Note however a significant anisotropic behaviour in the acquired signals, which indicates the presence of additional magnetic components possibly attributable to locally twisted graphene sublattices (for lamella layers-orientation perpendicular to the applied field).